Int. J. Electrochem. Sci., 9 **(2014)** 6580 - 6593

International Journal of
ELECTROCHEMICAL
SCIENCE
www.electrochemsci.org

Electrochemical and Theoretical Studies on Amino Phosphonates as Efficient Corrosion Inhibitor for N80 Steel in Hydrochloric Acid Solution

Mahendra Yadav[1,*], *Dipti Sharma*[1], *Sumit Kumar*[1], *Sushil Kumar*[1], *Indra Bahadur*[2,3], *Eno E. Ebenso*[2,3,*]

[1] Department of Applied Chemistry, Indian School of Mines, Dhanbad, 826004, India
[2] Department of Chemistry, North-West University (Mafikeng Campus), Private Bag X2046, Mmabatho 2735, South Africa
[3] Material Science Innovation & Modelling (MaSIM) Research Focus Area, Faculty of Agriculture, Science and Technology, North-West University (Mafikeng Campus), Private Bag X2046, Mmabatho 2735, South Africa
[*]E-mail: yadav_drmahendra@yahoo.co.in; Eno.Ebenso@nwu.ac.za

Received: 28 June 2014 / *Accepted:* 9 August 2014 / *Published:* 25 August 2014

Amino phosphonate compounds, namely, dimethyl-(4-methoxyphenyl) (phenylamino) methyl phosphonate (DMMP) and dimethyl phenyl (phenylamino)methylphosphonate (DPMP) were synthesized and studied as inhibitors for N80 steel corrosion in 15% HCl solution using the potentiodynamic polarization and electrochemical impedance spectroscopy (EIS) techniques. Polarization studies showed that both studied inhibitors were of mixed type in nature. The adsorption of inhibitors on the N80 steel surface obey Langmuir adsorption isotherm. Scanning electron microscopy (SEM), energy dispersive X-ray spectroscopy (EDX), and atomic force microscopy (AFM) were performed for surface study of uninhibited and inhibited N80 steel samples. Density functional theory (DFT) was employed for theoretical calculations.

Keywords: N80 steel; Corrosion inhibition; Phosphonates; EIS; Density functional theory

1. INTRODUCTION

Phosphonates are effective chelating agents. That is, they bind tightly to di- and trivalent metal ions, which is useful in water softening. In this way, they prevent formation of insoluble precipitates (scale). They are stable under harsh conditions. For these reasons, an important industrial use of phosphonates is in cooling waters, desalination systems, and in oil fields to inhibit scale formation. Phosphonates in cooling water systems also serve to control corrosion of iron and steel. Phosphonates

are also used in various industrial processes such as desalination, pulp production & bleaching of paper and textiles. Phosphonates are also increasingly used in medicine to treat disorders associated with bone formation and calcium metabolism. Acid solutions widely used in various industrial processes such as oil well acidification, petrochemical processes, acid pickling, acid cleaning, and acid de-scaling, generally, leads to serious metallic corrosion. Acidification of petroleum oil well for enhancing oil production is commonly carried out by forcing a solution of 15% to 28% hydrochloric acid into the well through N80 steel tubing. During this process N80 tubing get adversely affected by corrosion, therefore, to reduce the aggressive attack of the acid on tubing and casing materials (N80 steel), inhibitors are added to the acid solution during the acidifying process [1-4]. Organic compounds containing electronegative groups, triple bonds or conjugated double bonds are most efficient organic inhibitors because of their nucleophilicity and the capability to bind the metal surface by means of π-interaction [5-9]. The presence of heteroatoms such as nitrogen, sulphur, phosphorus, and oxygen, together with aromatic rings in the structure enhances the adsorption capability of the molecules on the metal surface and improve the corrosion inhibition efficiency of these compounds [10-13].

In continuation of our research for developing corrosion inhibitors [1-3] with high effectiveness and efficiency, in the present investigation we have synthesized Amino phosphonate compounds, namely, dimethyl-(4-methoxyphenyl) (phenylamino)methylphosphonate (DMMP) and dimethyl phenyl (phenylamino)methylphosphonate (DPMP) and studied their corrosion inhibition properties on N80 steel in 15% HCl solution by using potentiodynamic polarization, AC impedance, SEM, EDX, AFM and quantum chemical calculations.

2. EXPERIMENTAL PROCEDURES

2.1. Synthesis of inhibitor compounds

The inhibitors were synthesized by the method reported in literature [14] as shown in Scheme 1. Purity of DMMP and DPMP compounds was checked by thin layer chromatography (TLC) on silica gel G using chloroform: methanol (8:2) solvent system.

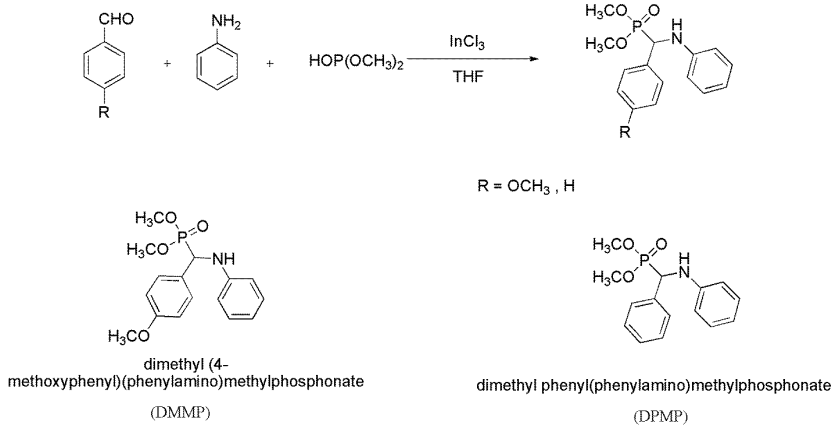

Scheme 1. Synthetic route and structure of dimethyl-(4-methoxyphenyl) (phenylamino)methylphosphonate (DMMP) and dimethyl phenyl (phenylamino)methylphosphonate (DPMP).

2.2. N80 steel sample

Corrosion studies were performed on N80 steel samples having composition (wt %): C, 0.31; Mn, 0.92; Si, 0.19; S, 0.008; P, 0.010; Cr, 0.20 and Fe balance. N80 Steel samples having dimension 1.0 cm × 1.0 cm × 0.1 cm with an exposed area of 1 cm^2 (rest covered with araldite resin) with 3 cm long stem were used for polarization and AC impedance experiment.

2.3. Test solution

The test solutions (15% HCl solution) were prepared by dilution of analytical grade 37% HCl with distilled water. The volume of test solution used for electrochemical studies was 150 mL. The concentrations of the studied inhibitors ranged from 25 ppm to 200 ppm by weight in 15% HCl solution.

2.4. Methods

2.4.1. Polarization and electrochemical impedance spectroscopy method

Electrochemical measurements were conducted in a conventional three-electrode cell consisting of N80 steel sample of 1 cm^2 exposed area as working electrode, a platinum counter electrode and a saturated calomel electrode (SCE) as reference electrode, using CH electrochemical workstation (Model No: CHI 760D, manufactured by CH Instruments, Austin, USA) at 303 K. Before polarization and impedance measurements, the working electrode was immersed in the test solution until a steady-state of the open-circuit potential was obtained. Potentiodynamic polarization curves were obtained at the scan rate of 1.0 mVs^{-1} in the potential range from +300 to -300 mV vs SCE with respect to open circuit potential. Corrosion current density (i_{corr}) was obtained by Tafel extrapolation method.

Electrochemical impedance measurements were carried out using AC signals of amplitude 10 mV peak to peak at the open circuit potential in the frequency range100 kHz to 10 mHz. All impedance data were fitted to appropriate circuits using ZSimpWin.3.21 software.

2.4.2. Scanning electron microscopic and energy dispersive spectroscopy analysis

The SEM and EDX images of polished, uninhibited and inhibited N80 steel samples were carried out using the instrument, Model: S-3400N, Make: Hitachi, Japan.

2.4.3. Atomic Force Microscopy

The AFM images of polished, uninhibited and inhibited N80 steel samples were carried out using a Nanosurf Easyscan2 instrument, Model: NT-MDT, Russia; Solver Pro-47.

2.4.4. Quantum chemical study

Quantum chemical calculations were performed using density functional theory (DFT) with the Beck's three parameter exchange functional along with the Lee–Yang–Parr nonlocal correlation functional (B3LYP) with 6-31G (d, p) basis set implemented in Gaussian 03 program package [15,16]. Theoretical parameters such as the energies of the highest occupied and lowest unoccupied molecular orbital (E_{HOMO} and E_{LUMO}), energy gap (ΔE) and dipole moment (μ) were determined.

3. RESULTS AND DISCUSSION

3.1. Polarisation studies

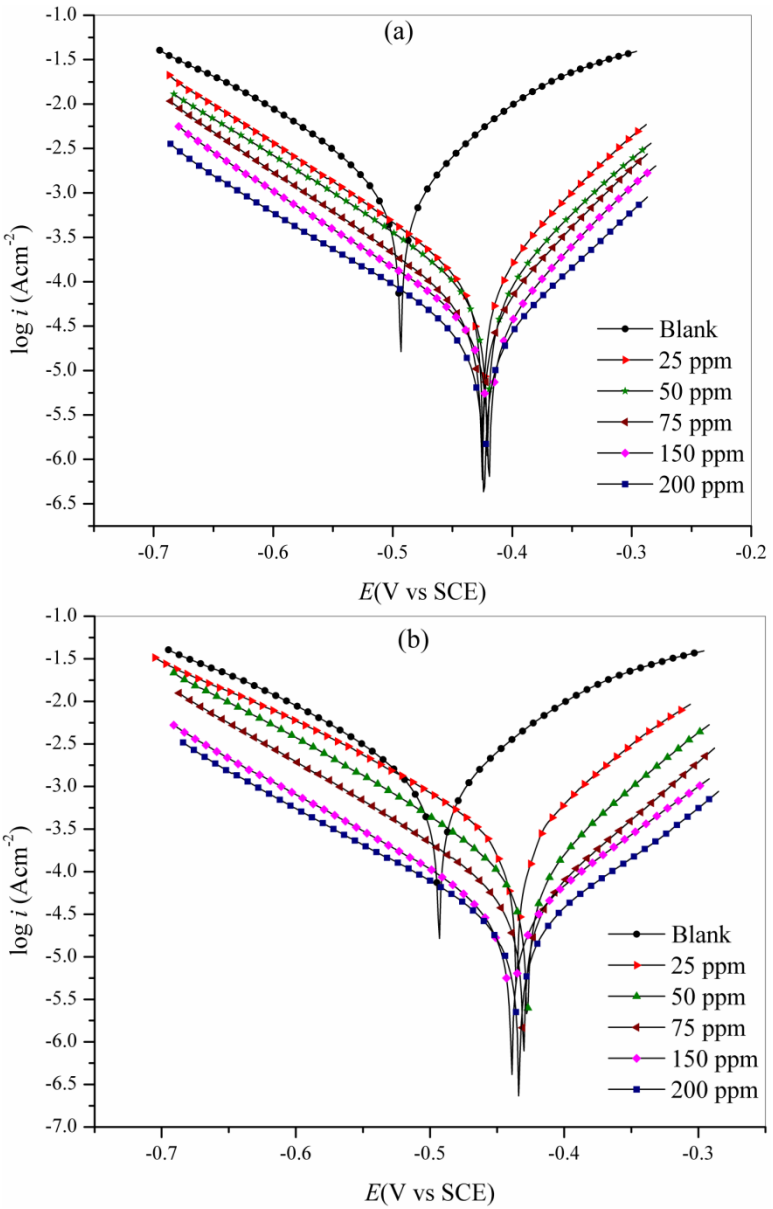

Figure 1. Potentiodynamic polarization curves for N80 steel in 15% HCl solution in the presence and absence of inhibitor at 303K (a) DMMP (b) DPMP.

The effect of inhibitors concentration on the anodic and cathodic polarization behavior of N80 steel in 15% HCl solution has been studied by polarization measurements and the recorded Tafel plots for different inhibitors (DMMP and DPMP) at studied concentrations are shown in Figure 1 (a, b) at 303 K. The corrosion parameters such as corrosion potential (E_{corr}), anodic Tafel slope (β_a), cathodic Tafel slope (β_c) and corrosion current density (i_{corr}) obtained from these curves are given in Table 1. The percentage inhibition efficiency (η%) was calculated using the equations given below:

$$\eta(\%) = \frac{i^0_{corr} - i_{corr}}{i^0_{corr}} \times 100 \quad (1)$$

where, i^0_{corr} and i_{corr} are the values of corrosion current density in absence and presence of inhibitors, respectively.

It is illustrated from the Figure 1 (a, b), that both anodic metal dissolution of iron and cathodic hydrogen evolution reaction were inhibited after the addition of inhibitors to 15% HCl solution. The inhibition of these reactions was more pronounced on increasing inhibitors concentration. The lower corrosion current density (i_{corr}) values in the presence of inhibitor without causing significant changes in corrosion potential suggests that, the inhibitors are mixed type inhibitor (i.e., inhibits both anodic and cathodic reactions) and is adsorbed on the surface, thereby blocking the corrosion reaction [17-19]. The anodic Tafel slope (β_a) and the cathodic Tafel slope (β_c) of DMMP and DPMP changed with inhibitor concentration, indicating that these inhibitors controlled both anodic as well as cathodic reactions. The minor shift in E_{corr} towards positive potential for both the inhibitors indicated that these inhibitors act as mixed inhibitor with more tendencies towards anodic nature.

3.2. EIS studies

EIS measurements were performed to determine the impedance parameters of the N80 steel/hydrochloric acid interface in the absence and presence of various concentrations of inhibitors. Adsorption of a protective inhibitor on the metal surface causes a significant increase in impedance of the corrosion system, thus causing an increase in the resistance to charge transfer process. Therefore, the performance of an inhibitor can be determined by impedance measurements of the corrosion system. The degree of the corrosion protection can be determined by comparing the impedance obtained in the presence and absence of inhibitors in the corrosive environment. The Nyquist plots for N80 steel obtained at N80 steel / 15% HCl solution interface with and without the different concentrations of DMMP and DPMP at 303 K are shown in Figure 2 (a, b).The existence of a depressed semicircle with its center below the axis ($Z^{'}$) in Nyquist plots (Fig.2 a, b) for both inhibitors suggesting the non-homogeneity and roughness of the N80 steel surface [20]. The EIS spectra of all tests were analyzed using the equivalent circuit shown in Figure 3, which is a parallel combination of the charge transfer resistance (R_{ct}) and the constant phase element (CPE), both in series with the solution resistance (R_s). This type of electrochemical equivalent circuit was reported previously to model the iron/acid interface [21]. Constant phase element (CPE) is introduced instead of pure double layer capacitance to give more accurate fit as the double layer at interface does not behave as ideal capacitor.

The electrochemical parameters such as solution resistance, charge transfer resistance and CPE constants (Y_0 and n) obtained from the fitting the experimental data of Nyquist plots in the equivalent circuit shown in Fig. 3 are presented in Table 1.

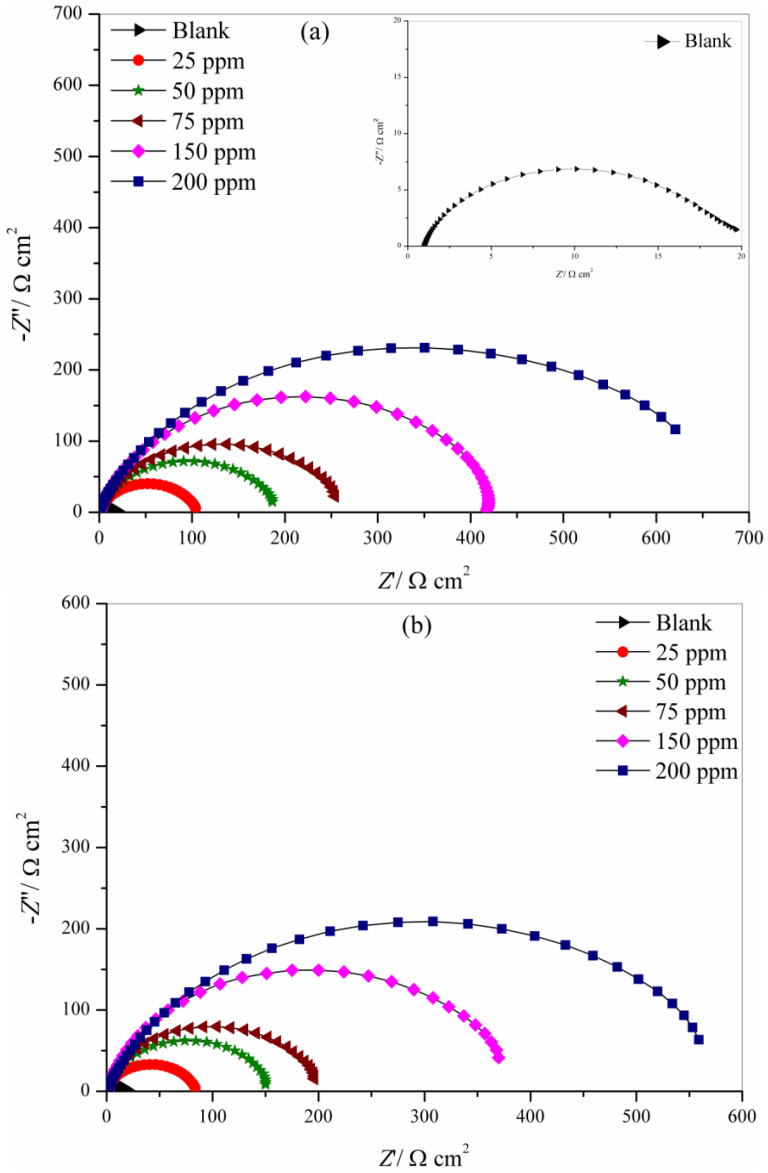

Figure 2. Nyquist plot for N80 steel in 15% HCl solution in the presence and absence of inhibitor at 303K (a) DMMP (b) DPMP.

The inhibition efficiency (η %) was calculated from charge transfer resistance values obtained from impedance measurements using the following relation

$$\eta(\%) = \frac{R_{ct\,(inh)} - R_{ct}}{R_{ct\,(inh)}} \times 100 \qquad (2)$$

where $R_{ct(inh)}$ and R_{ct} are charge transfer resistance in presence and absence of inhibitor respectively.

The value of double layer capacitance (C_{dl}) were calculated from charge transfer resistance and CPE parameters (Y_0 and n) using the expression [22].

$$C_{dl} = (Y_0 R_{ct}^{1-n})^{1/n} \qquad (3)$$

where Y_0 is CPE constant and n is CPE exponent. The value of n represents the deviation from the ideal behavior and it lies between 0 and 1.

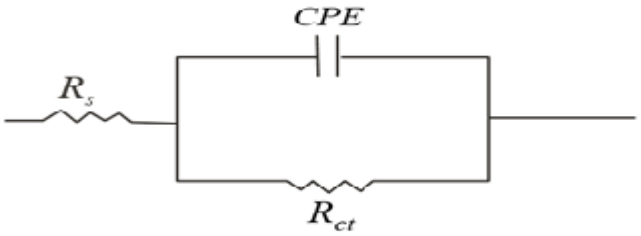

Figure 3. Equivalent circuit applied for fitting of the impedance spectra.

The data shown in Table 1 reveal that the value of R_{ct} increases with addition of inhibitors as compared to the blank solution, the increase in R_{ct} value is attributed to the formation of a protective film at the metal/solution interface. The C_{dl} value decreases on increasing the concentration of both the inhibitors, indicating the decrease in local dielectric constant and/or to an increase in the thickness of the electrical double layer, suggesting that the inhibitor molecules are adsorbed at the metal/solution interface.

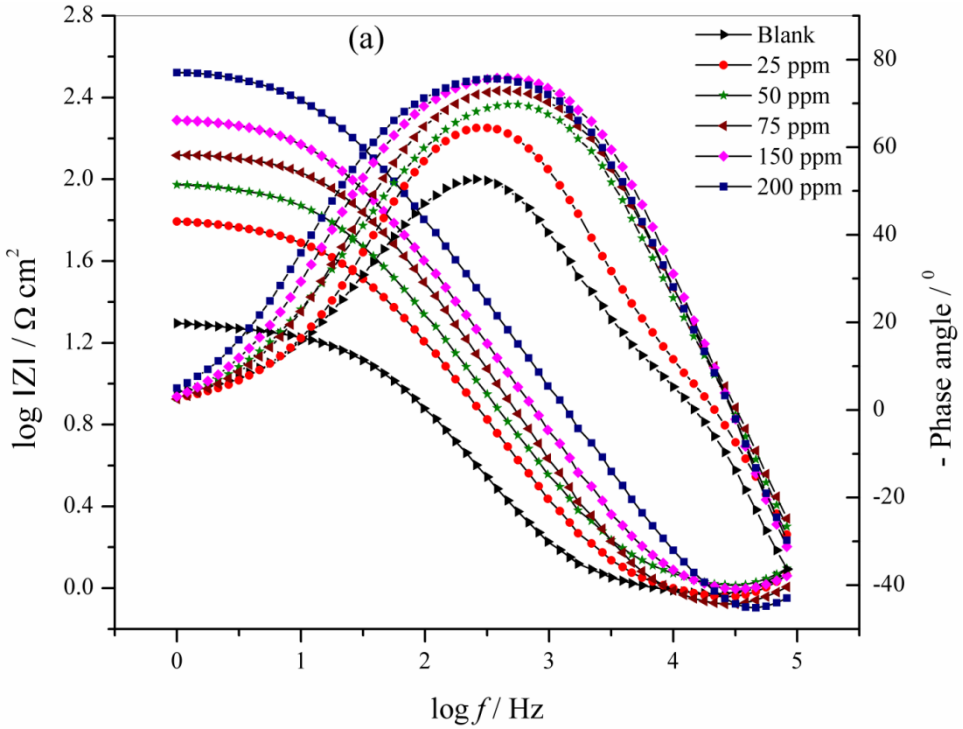

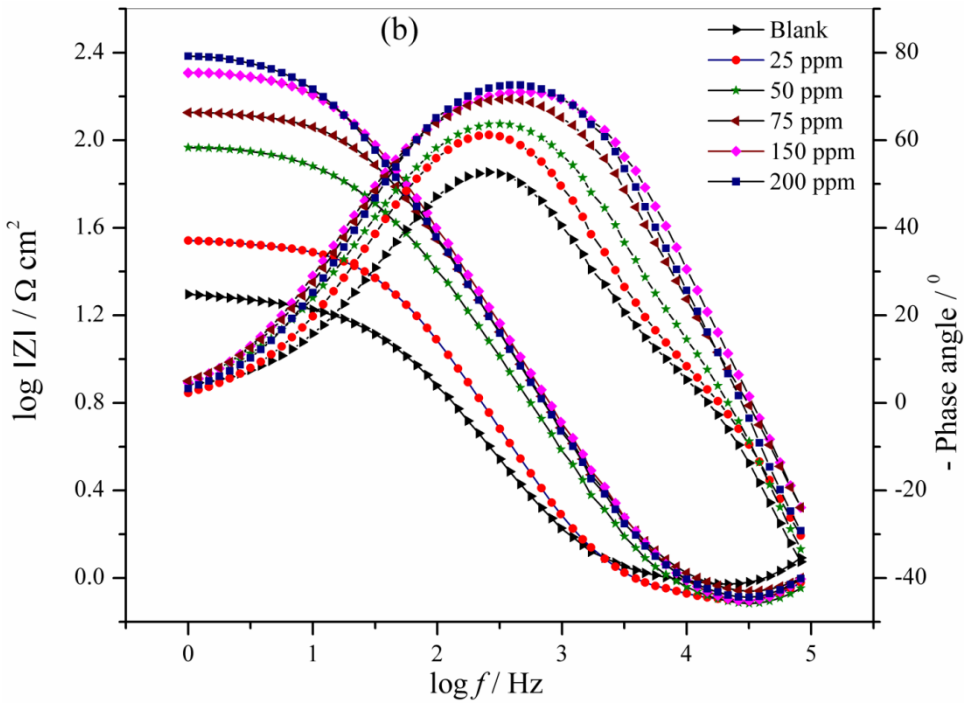

Figure 4. Bode plots for N80 steel in 15% HCl solution in the absence and presence of different concentrations of inhibitors (a) DMMP (b) DPMP.

Table 1. Electrochemical parameters and percentage inhibition efficiency (*η %)* obtained from polarization studies for N80 steel in 15% HCl solution in the presence and absence of inhibitor at 303 K.

Conc. (ppm)	Tafel extrapolation data					EIS data					
	E_{corr} (V vs SCE)	β_a (mV dec^{-1})	β_c (mV dec^{-1})	I_{corr} (μAcm^{-2})	η %	R_s (Ω cm^2)	R_{ct} (Ω cm^2)	Y_0 (μFcm^{-2})	n	C_{dl} (μF cm^2)	η %
Blank	-495	93	142	568	-	0.93	20	573	0.845	252	-
DMMP											
25	-432	105	178	112.4	80.2	0.74	106	172	0.868	93.3	81.1
50	-428	112	169	75.5	86.7	0.88	188	114	0.885	69.4	89.3
75	-430	96	156	51.1	91.0	0.62	263	85	0.892	53.6	92.4
150	-422	107	163	39.2	93.1	0.73	418	50	0.904	33.1	95.2
200	-418	88	158	25.0	95.6	0.54	700	24	0.942	18.7	97.2
DPMP											
25	-424	98	167	124.9	78.0	0.58	87	196	0.862	102.1	77.0
50	-438	117	183	84.0	85.2	0.87	154	143	0.871	81.2	87.0
75	-432	108	148	65.3	88.5	0.91	202	107	0.883	64.4	90.1
150	-427	86	172	43.1	92.4	0.78	386	66	0.892	42.3	94.8
200	-423	102	162	34.6	93.9	0.82	596	35	0.933	26.5	96.6

The single peak obtained in Bode plots (Fig.4 a, b) for both inhibitors indicates that the electrochemical impedance measurements were fit well in one time constant equivalent model with constant phase element (CPE). Moreover, there is only one phase maximum in Bode plot (Fig.4 a, b)

for both inhibitors, indicates only one relaxation process, which would be the charge transfer process, taking place at the metal- electrolyte interface. Figure 4 (a, b) show that the impedance value in the presence of both inhibitors is larger than in absence of inhibitors and the value of impedance increases on increasing the concentration of both studied inhibitors. These mean that the corrosion rate is reduced in presence of the inhibitors and continued to decreasing on increasing the concentration of inhibitors.

3.3. Scanning electron microscopy

The surface morphology of the N80 steel samples in 15% HCl solution in the absence and presence of 200 ppm of DMMP and DPMP are shown in Figure 5 (a, b c, d). Figure 5 (a) is SEM of N80 steel sample before immersion in 15% HCl solution. The badly damaged surface (Fig. 5 b) obtained when the metal was kept immersed in 15% HCl solution for 6 h without inhibitor indicates significant corrosion. However, in presence of inhibitors (Figs. 5 c, d) the surface has remarkably improved with respect to its smoothness indicating considerable reduction of corrosion rate. This improvement in surface morphology is due to the formation of a good protective film of inhibitor on N80 steel surface which is responsible for inhibition of corrosion.

3.4. Energy dispersive X-ray spectroscopy

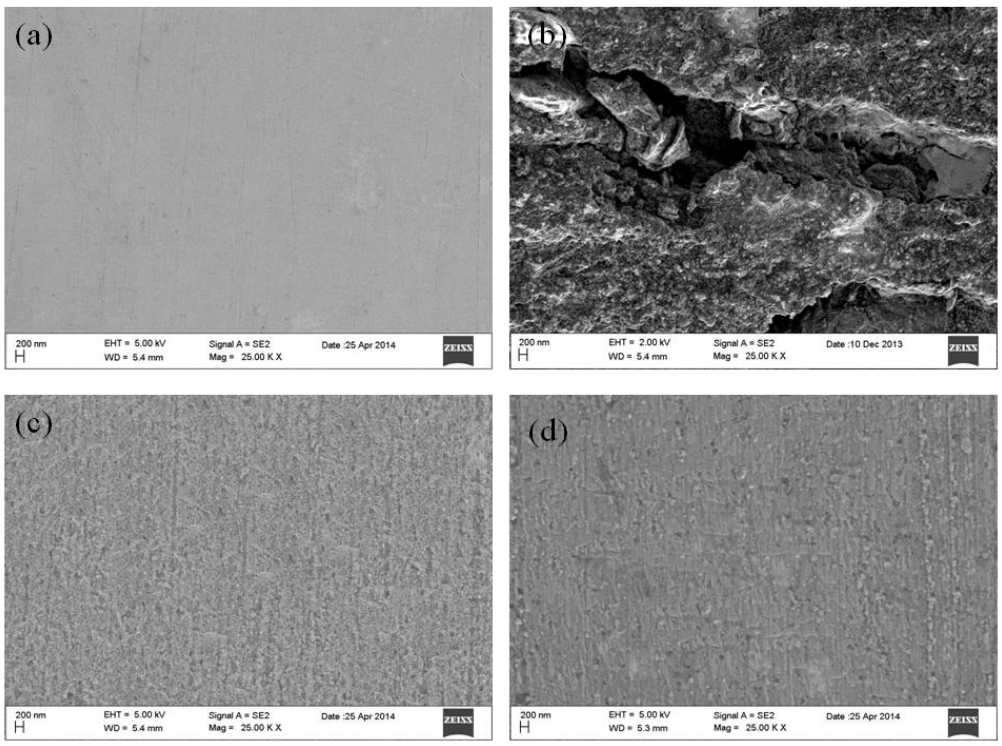

Figure 5. SEM image of N80 steel (a) before immersion (polished) (b) After immersion without inhibitor (c) in presence of inhibitor DMMP (d) in presence of inhibitor DPMP.

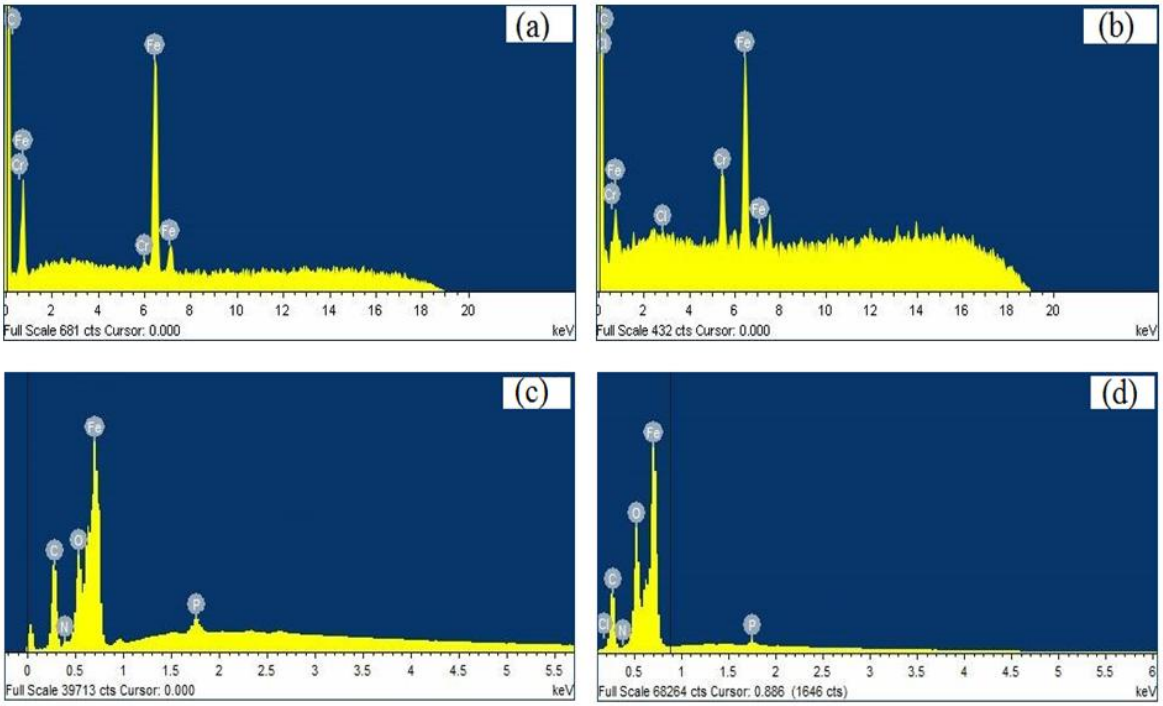

Figure 6. EDX spectra of N80 steel specimens (a) polished (b) After immersion without inhibitor (c) with 200 ppm DMMP (d) with 200 ppm DPMP.

The results of EDX spectra are shown in Figure 6 (a, b, c, d). Figures 6 (a) and (b) represent the EDX spectra of abraded and uninhibited N80 steel specimen and Figures 6 (c) and (d) depicts inhibited N80 steel specimens. The abraded N80 steel specimen shows characteristic peaks of elements (C, Mn, Cr, Fe) constituting N80 steel sample. The EDX spectra of uninhibited N80 steel (Fig. 6 b) shows a peak corresponding to Cl in addition to the abraded sample peaks. The EDS spectra of inhibited N80 steel contains the peaks corresponding to all the elements present in the inhibitor molecules indicating the adsorption of inhibitor molecules at the surface of N80 steel. In addition to that, EDX of inhibited spectra shows that the Fe peaks are considerably suppressed as compared to abraded and uninhibited N80 steel sample. The suppression of Fe lines might be due to overlying inhibitor film. This indicated that N80 steel surface was covered with protective film of inhibitor molecules.

3.5. Atomic force microscopy

Surface morphology of the polished N80 steel sample and N80 steel sample in 15% HCl solution in absence and presence of inhibitors were investigated by atomic force microscopy (AFM). The results are shown in Figure 7 (a–d). The average roughness of polished N80 steel sample (Fig. 7 a) and N80 steel sample in 15% HCl solution without inhibitor (Fig. 7 b) were found as 25 and 650 nm. It is clearly shown in Figure 7 (b) that N80 steel sample is badly damaged due to the acid attack on surface. However, in presence of optimum concentration (250 ppm) of DMMP and DPMP as shown in Figure 7 (c, d), the average roughness were reduced to 95 and 130 nm, respectively. The decrease in

roughness in presence of inhibitors is due to adsorption of inhibitors at the surface of N80 steel. The lower value of roughness for DMMP than DPMP reveals that DMMP protects the N80 steel surface more efficiently than DPMP in 15% HCl solution.

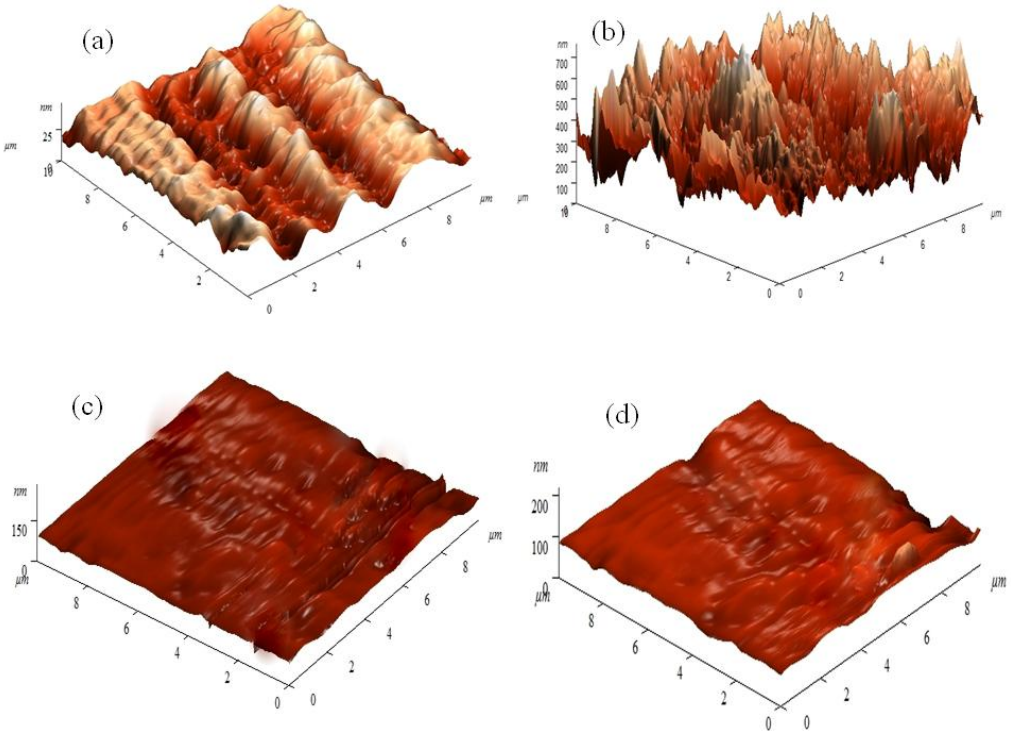

Figure 7. AFM micrograph of N80 steel surface (a) polished N80 steel (b) blank 15 % HCl solution (c) 15 % HCl solution with 200 ppm DPMP (d) 15 % HCl solution with 200 ppm DMMP.

3.6. Theoretical studies

The optimized structure, E_{HOMO} and E_{LUMO} of both the inhibitors are shown in Figure 8 (a, b). The quantum chemical parameters such as the energy of the highest occupied molecular orbital (E_{HOMO}), the energy of the lowest unoccupied molecular orbital (E_{LUMO}), energy gap (ΔE) and dipole moment (μ) were determined using DFT. According to the frontier molecular orbital (FMO) theory of chemical reactivity, the formation of a transition state is due to interaction between HOMO and LUMO of reacting species. It was reported previously by some researchers that smaller values of ΔE and higher values of dipole moment (μ) are responsible for higher inhibition efficiency [23] of inhibitors. According to HSAB theory hard acids prefer to co-ordinate to hard bases and soft acid to soft bases. Fe is considered as soft acid and will co-ordinate to molecule having maximum softness and small energy gap ($\Delta E = E_{LUMO} - E_{HOMO}$). For DMMP the values of E_{HOMO}, E_{LUMO} , ΔE and μ were found as – 5.203, -0.0838, 5.119 and 1.861 respectively, whereas for DPMP the values for E_{HOMO}, E_{LUMO} , ΔE and μ were found as – 5.266, -0.0925, 5.173 and 1.432 respectively. The higher value of

E_{HOMO}, μ and lower values of E_{LUMO} and ΔE for DMMP indicated that DMMP has more potency to get adsorbed on the N80 steel surface resulting greater inhibition tendency than DPMP.

Figure 8 (a, b), reveals that the HOMO and LUMO location in both inhibitors is mostly distributed in vicinity of the nitrogen and phosphorous These indicate the reactive sites of the inhibitors for adsorption at the surface of N80 steel surface.

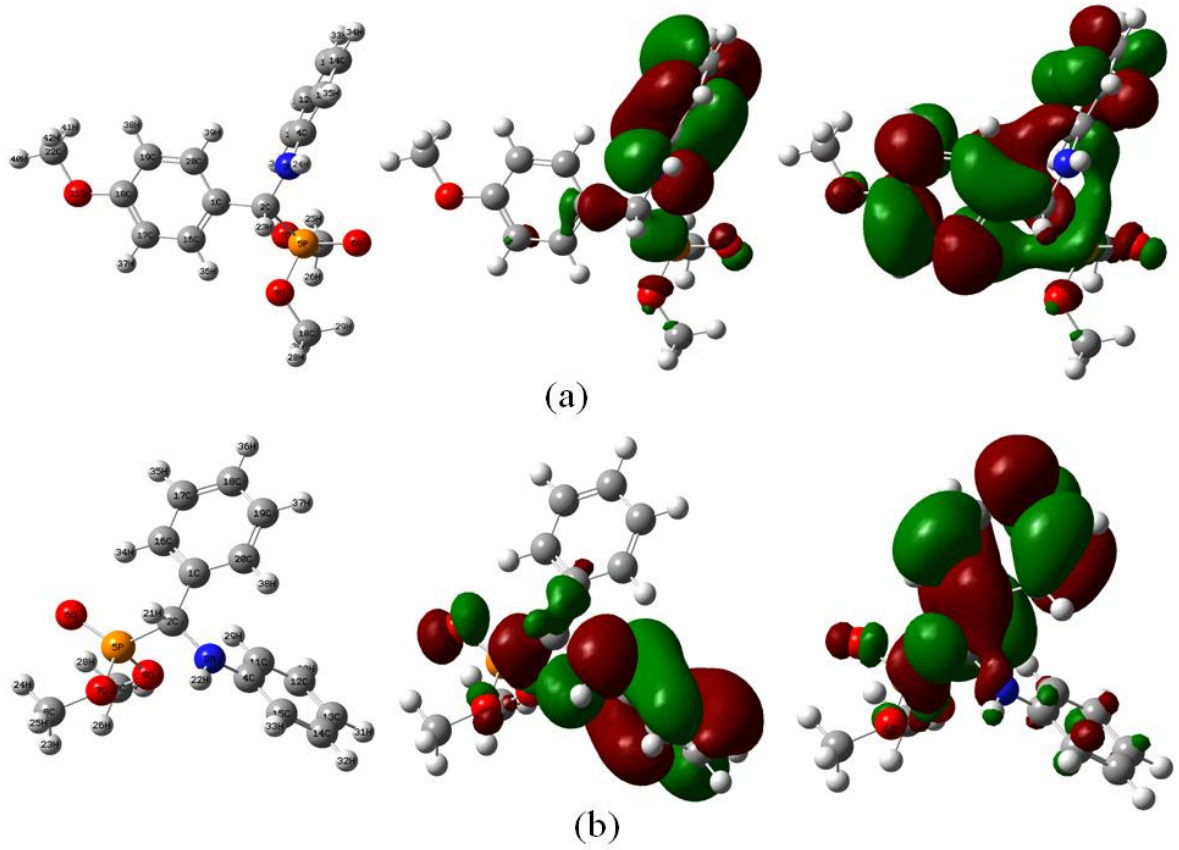

Figure 8. The optimized structure (left) and HOMO (center) and LUMO (right) distribution for molecules (a) DMMP (b) DPMP. [Atom legend: white = H; Cyan = C; blue = N; red = O; Orange = P].

3.7. Mechanism of inhibition

Corrosion inhibition of N80 steel in 15% hydrochloric acid solution by both inhibitors (DMMP and DPMP) can be explained on the basis of molecular adsorption. These compounds inhibit corrosion by controlling both anodic as well as cathodic reactions. In 15% hydrochloric acid solutions these inhibitors exist as protonated species. In both inhibitors the nitrogen atoms present in the molecules can be easily protonated in acidic solution and convert into quaternary compounds. These protonated species adsorbed on the cathodic sites of the N80 steel and decrease the evolution of hydrogen. The adsorption on anodic site of the metal occurs through π-electrons of phenyl rings and lone pair of electrons of nitrogen, phosphorous and oxygen atoms present in both the inhibitors decreases the anodic dissolution of N80 steel [24, 25].

4. CONCLUSIONS

(1) The synthesized amino phosphonate compounds showed good inhibition efficiencies for the corrosion of N80 steel in 15% HCl solution and the inhibition efficiency increased on increasing the concentration of inhibitor. The inhibiting performance of DMMP is better than DPMP.

(2) EIS measurements show that charge transfer resistance (R_{ct}) increases and double layer capacitance (C_{dl}) decreases in presence of inhibitors, suggested the adsorption of the inhibitor molecules on the surface of N80 steel.

(3) It is suggested from the results obtained from AFM that the mechanism of corrosion inhibition is occurring mainly through adsorption process.

(4) Quantum chemical results of DMMP and DPMP show higher value of E_{HOMO}, lower value of E_{LUMO}, and smaller value of ΔE, indicating that both inhibitors are good corrosion inhibitor for N80 steel in hydrochloric acid.

ACKNOWLEDGEMENTS
The authors gratefully acknowledge North-West University , Department of Science and Technology and the National Research Foundation (DST/NRF) South Africa grant funded (Grant UID: 92333) for postdoctoral scholarship of Dr I. Bahadur.

References

1. M. Yadav, D. Behera, U. Sharma, *Corros. Eng. Sci. Technol.*, 48 (2013) 19.
2. M. Yadav, D. Behera, U. Sharma *Arab. J. Chem.* DOI: 10.1016/j.arabjc.2012.03.011.
3. M. Yadav, U. Sharma, *J. Mater. Environ. Sci.*, 2 (2011) 407.
4. S. Vishwanatham, P.K. Sinha, *Anti-Corros. Methods Mater*, 56 (2009) 139.
5. J. Cruz, R. Martinez, J. Genesca, E. Garcia-Ochoa, *J. Electroanal. Chem*., 566 (2004) 111.
6. A.M.S. Abdennaby, A.I. Abdulhady, S.T. Abu-Oribi, H. Saricimen, *Corros. Sci*., 38 (1996) 1791.
7. S. Kertit, B. Hammouti, *Appl. Surf. Sci*., 93 (1996) 59.
8. K.D. Neemla, A. Jayaraman, R.C. Saxena, A.K. Agrawal, R. Krishna, *Bull. Electrochem.*, 5 (1989) 250.
9. R.M. Hudson, T.J. Bulter, C.J. Warning, *Corros. Sci*., 17 (1977) 571.
10. M. Bouklah, A. Ouassini, B. Hammouti, A. El Idrissi, *Appl. Surf. Sci*., 250 (2005) 50.
11. P.B. Raja, M.G. Sethuraman, *Mater. Lett*., 62 (2008) 113.
12. A.Y. El-Etre, *Corros. Sci*., 45 (2003) 2485.
13. A.M. Abdel-Gaber, B.A. Abd-El-Nabey, M. Saadawy, *Corros. Sci*., 51 (2009) 1038.
14. B. C. Ranu, A. Hajra, U. Jana, *Org. Lett.*, 1 (1999) 1141.
15. C. Lee, W. Yang, R.G. Parr, *Phys. Rev*., B 37 (1988) 785.
16. A. D. Becke, *J. Chem. Phys.*, 98 (1993) 1372.
17. X. Wang, H. Yang, F. Wang, *Corros. Sci.*, 53 (2011) 113.
18. D. Jayaperumal, *Mater. Chem. Phys.*, 119 (2010) 478.
19. E. S. Ferreira, C. Giancomlli, F. C. Giacomlli, A. Spinelli, *Mater. Chem. Phys*., 83 (2004) 129.
20. M. Lebrini, M. Lagrene´e, H. Vezin, M. Traisnel, F. Bentiss, *Corros. Sci*., 49 (2007) 2254.
21. H. Gerengi, H.I. Sahin, *Ind. Eng. Chem. Res.*, 51 (2012) 780.
22. M. Lebrini, F. Robert, A. Lecante, C. Roos, *Corros. Sci.*, 53 (2011) 687.

23. V.S. Sastri, J.R. Perumareddi, *Corrosion*, 53 (1997) 617.
24. N.O. Obi-Egbedi, K.E. Essien, I.B. Obot, E.E. Ebenso, *Int. J. Electrochem. Sci.* 6 (2011) 913.
25. I.B. Obot, N.O. Obi-Egbedi, S.A. Umoren, *Int. J. Electrochem. Sci.* 4 (2009) 863.